acetate, pH 4.8. After addition of 1/10 volume 5*M* sodium acetate, pH 5.8, the resulting RNA was precipitated from the aqueous phase with two volumes of 100% ethanol. The RNA precipitate was collected by centrifugation, washed in 70% ethanol, and dried briefly prior to first strand cDNA synthesis by random priming and a commercially available kit (Boehringer Mannheim, Indianapolis, IN). After the completion of second strand synthesis, aliquots of the cDNA were modified by addition of Eco RI linkers (New England Biolabs, Beverly, MA) for the construction of cDNA libraries in the phage vector λgt10 (Promega Biotec, Madison, WI). The initial λgt10 library contained 9.1×10^6 apparent recombinant plaques when titered on the *Escherichia coli* hfl strain HG415. Analysis of random plaque pure clones indicated, however, that the actual recombinant frequency was less than 5%. This library was, therefore, plated and total phage DNA was prepared. The phage DNA was cleaved with Eco RI, fractionated on agarose gels, and inserts in the 500- to 4000-bp size range were recovered on NA45 paper for recloning into λgt10. This resulted in a library with a recombinant frequency of greater than 90%.

10. J. P. Kim *et al.*, unpublished data.
11. R. Sager, A. Anisowicz, N. Howell, *Cell* **23**, 41 (1981).
12. G. R. Reyes *et al.*, in *Viral Hepatitis and Hepatocellular Carcinoma*, J. L. Sung and D.-S. Chen, Eds. (Excerpta Medica, New York, in press).
13. K. Fry *et al.*, in preparation.
14. R. K. Saiki *et al.*, *Science* **230**, 1350 (1985); K. B. Mullis and F. A. Faloona, *Methods Enzymol.* **155**, 335 (1987).
15. R. K. Saiki *et al.*, *Science* **239**, 487 (1988).
16. G. R. Reyes and J. P. Kim, in preparation; J. P. Kim *et al.*, *J. Cell. Biochem. Suppl. 13E* **WH160**, 293 (1989).
17. E. M. Southern, *J. Mol. Biol.* **98**, 503 (1975).
18. D. W. Bradley *et al.*, in *Viral Hepatitis and Liver Disease*, H. A. Zuckerman, Ed. (Liss, New York, 1988), pp. 138–147; K. M. DeCock *et al.*, *Ann. Int. Med.* **106**, 227 (1987).
19. W. R. Pearson and D. J. Lipman, *Proc. Natl. Acad. Sci. U.S.A.* **85**, 2444 (1988).
20. G. Kamer and P. Argos, *Nucleic Acids Res.* **12**, 7269 (1984).
21. Software available from Intelligenetics, Mountain View, CA.
22. G. Reyes *et al.*, unpublished observations.
23. R. H. Purcell and J. R. Ticehurst, in *Viral Hepatitis and Liver Disease*, H. A. Zuckerman, Ed. (Liss, New York, 1988), pp. 131–137.
24. D. W. Bradley *et al.*, *J. Gen. Virol.* **69**, 731 (1988).
25. D. N. Love and M. Sabine, *Arch. Virol.* **48**, 213 (1975).
26. F. L. Schaffer, *Comp. Virol.* **14**, 249 (1979).
27. D. Bradley, unpublished observations.
28. V. A. Arankalle *et al.*, *Lancet* **i**, 550 (1988).
29. F. Sanger, S. Nicklen, A. R. Coulson, *Proc. Natl. Acad. Sci. U.S.A.* **74**, 5463 (1979).
30. D. W. Mount and B. Conrad, *Manual for Computer Programs for DNA and Protein Sequence Analysis, Version 4.2* (Univ. of Arizona, Tucson, 1986). Abbreviations for the amino acid residues are: A, Ala; C, Cys; D, Asp; E, Glu; F, Phe; G, Gly; H, His; I, Ile; K, Lys; L, Leu; M, Met; N, Asn; P, Pro; Q, Gln; R, Arg; S, Ser; T, Thr; V, Val; W, Trp; and Y, Tyr.
31. M. Houghton, Q.-L. Choo, G. Kuo, European Patent Application #88310922.5, 5/31/89 Bulletin 89/22.
32. J. I. Cohen, J. R. Ticehurst, R. H. Purcell, A. Buckler-White, B. Baroudy, *J. Virol.* **61**, 50 (1987).
33. H. Sumiyoshi *et al.*, *Virology* **161**, 497 (1987).
34. A. Nomoto *et al.*, *Proc. Natl. Acad. Sci. U.S.A.* **79**, 5793 (1982).
35. A. R. Carrol, D. J. Rowlands, B. E. Clarke, *Nucleic Acids. Res.* **12**, 2461 (1984).
36. A. C. Palmenberg *et al.*, *ibid.*, p. 2969.
37. E. G. Strauss *et al.*, *Virology* **133**, 92 (1984).
38. P. Goelet *et al.*, *Proc. Natl. Acad. Sci. U.S.A.* **79**, 5818 (1982).
39. B. J. C. Cornilissen, F. T. Brederode, G. H. Veeneman, J. H. van Boom, J. F. Bol, *Nucleic Acids Res.* **11**, 3019 (1983).
40. P. Ahlquist, R. Dasgupta, P. Kraesberg, *Cell* **23**, 183 (1981).
41. G. B. Lomonosoff and M. Shanks, *EMBO J.* **2**, 221 (1983).
42. P. Chomczynski and N. Sacchi, *Anal. Biochem.* **162**, 156 (1987).
43. H. Lehrach *et al.*, *Biochemistry* **16**, 4743 (1977).
44. We would like to thank our colleagues, J. Lifson and M. Lovett, for their thoughtful reading and helpful comments on the manuscript. The assistance of R. Sunshine, J. Fernandez, K. McCaustland, and the Genelabs Visual Arts Department is also appreciated.

27 October 1989; accepted 26 January 1990

Calcium-Induced Movement of Troponin-I Relative to Actin in Skeletal Muscle Thin Filaments

TERENCE TAO,* BANG-JIAN GONG, PAUL C. LEAVIS

The role of troponin-I (the inhibitory subunit of troponin) in the regulation by Ca^{2+} of skeletal muscle contraction was investigated with resonance energy transfer and photo cross-linking techniques. The effect of Ca^{2+} on the proximity of troponin-I to actin in reconstituted rabbit skeletal thin filaments was determined. The distance between the cysteine residue at position 133 (Cys^{133}) of troponin-I and Cys^{374} of actin increases by approximately 15 angstroms on binding of Ca^{2+} to troponin-C. Also, troponin-I labeled at Cys^{133} with benzophenone-4-maleimide could be photo cross-linked to actin in the absence of Ca^{2+}, but not in its presence. These results suggest that troponin-I is attached to actin in the Ca^{2+}-free or relaxed state of muscle, and that it detaches from actin on Ca^{2+} activation of contraction. Thus, troponin-I may function as a Ca^{2+}-dependent molecular switch in regulation of skeletal muscle contraction.

CONTRACTION OF VERTEBRATE STRIated muscle is regulated by Ca^{2+} and requires the regulatory proteins troponin (Tn) and tropomyosin (Tm) (*1*). Troponin is composed of three subunits, the Ca^{2+}-binding (TnC), inhibitory (TnI), and Tm-binding (TnT) subunits. TnI inhibits actomyosin Mg^{2+}-dependent adenosine triphosphatase (Mg-ATPase) activity by itself (*2, 3*). It binds weakly to filamentous actin (F-actin) (*4, 5*) near the NH_2-terminus of actin (*6*) and more strongly to a complex of Tm and F-actin (Tm–F-actin); TnC reverses the binding of TnI to Tm–F-actin in the presence of Ca^{2+}, but not in its absence (*4, 5*). On the basis of these and other findings, a model for regulation by Ca^{2+} of skeletal muscle contraction has been proposed (*4, 7, 8*). This model postulates that in the relaxed state (absence of Ca^{2+}), TnI is attached to actin and anchors Tm in a position or state that inhibits one of the steps in the actin-myosin interaction cycle. In the activated state (presence of Ca^{2+}), the binding of Ca^{2+} to TnC causes TnI to detach from actin, with the result that the inhibitory effect of Tm is reversed. With the use of reconstituted rabbit skeletal muscle thin filaments composed of Tn, Tm, and F-actin, we have directly examined how TnI functions in the proposed mechanism of Ca^{2+} regulation.

TnI labeled at Cys^{133} with the fluorescent donor 1,5-IAEDANS [*N*-iodoacetyl-*N*′-(5-sulfo-1-naphthyl)ethylenediamine] and F-actin labeled at Cys^{374} with the nonfluorescent acceptor DAB-Mal (4-dimethylaminophenylazophenyl-4′-maleimide) were reconstituted with the other thin filament proteins to form the (TnC-TnI^{DAN}-TnT)–Tm–F-actin and (TnC-TnI^{DAN}-TnT)–Tm–F-$actin^{DAB}$ complexes (where TnI^{DAN} is donor-labeled TnI and F-$actin^{DAB}$ is acceptor-labeled F-actin). Resonance energy transfer distances were measured in these complexes in the following metal-bound states: (i) the Ca^{2+}-state, in which both the high- and low-affinity metal-binding sites of TnC are saturated with Ca^{2+}, simulating the in vivo activated state; (ii) the Mg^{2+}-state, in which only the high-affinity sites are occupied by Mg^{2+}, simulating the in vivo relaxed state; and (iii) the apo-state, in which none of the sites are occupied.

Our results show that the extent of resonance energy transfer is markedly Ca^{2+}-dependent (Fig. 1 and Tables 1 and 2), the transfer yield being significantly lower in the Ca^{2+}-saturated state than in either of the two Ca^{2+}-free states. Measurements carried out in the presence of both Ca^{2+} (0.2 m*M*) and Mg^{2+} (4 m*M*) yielded the same results as those carried out in the Ca^{2+}-state (*9*). If we assume that the orientation factor, κ^2, is the isotropically averaged value of 2/3, dis-

T. Tao, Department of Muscle Research, Boston Biomedical Research Institute, 20 Staniford, Street, Boston, MA 02114, and Department of Neurology, Harvard Medical School, Boston, MA 02115.
B.-J. Gong, Department of Muscle Research, Boston Biomedical Research Institute, Boston, MA 02114.
P. C. Leavis, Department of Muscle Research, Boston Biomedical Research Institute, Boston, MA 02114; Department of Neurology, Harvard Medical School, Boston, MA 02115; and Department of Physiology, Tufts University School of Medicine, Boston, MA 02111.

*To whom correspondence should be addressed.

tances of 57, 42, and 39 Å were obtained for the Ca^{2+}-, Mg^{2+}-, and apo-states, respectively. Thus, there is little or no change in the apparent interprobe distance when Mg^{2+} occupies the high-affinity sites of TnC, but the distance increases by ~15 Å when all the sites are occupied by Ca^{2+}.

The limiting anisotropy, A_0, of (TnC-TnI^{DAN}-TnT)–Tm–F-actin was determined as a function of metal binding by anisotropy decay measurements. The values obtained were 0.220, 0.191, and 0.214 in the Ca^{2+}-, Mg^{2+}-, and apo-states, respectively (*9*). They are virtually independent of metal binding, indicating that there is no large change in the rigidity of the TnI-bound donor when metal ions bind to TnC. The values are significantly lower than the theoretical maximum of 0.4, indicating considerable randomization of the donor transition moment, justifying the use of 2/3 as the value of κ^2. With the use of the formalism introduced by Stryer (*10*), and an average value of 0.218 for A_0, we obtained a value of 35.5° for θ, the half-angle of a cone within which the donor transition moment is assumed to rotate rapidly. This corresponds to a range of κ^2 values between 0.475 and 0.904, or a range of ~30% in the determined distances. In practice, this range should be smaller because in this treatment the randomization of the acceptor transition moment orientation is not taken into account. These results show that the attached donor has considerable flexibility and the extent of flexibility is not Ca^{2+}-dependent, suggesting that the observed change in apparent interprobe distance is not likely to be due to changes in the orientation factor.

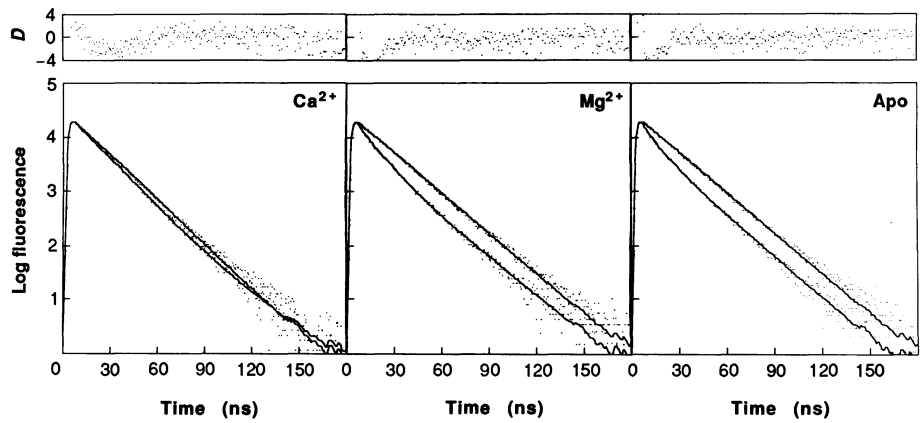

Fig. 1. Fluorescence decay curves of (TnC-TnI^{DAN}-TnT)–Tm–F-actin (upper curves) and (TnC-TnI^{DAN}-TnT)–Tm–F-$actin^{DAB}$ (lower curves) in the Ca^{2+}-, Mg^{2+}, and apo-states. Dots are experimental points. Solid lines are calculated fits with decay parameters derived from one-exponential [for (TnC-TnI^{DAN}-TnT)–Tm–F-actin] or two-exponential [for (TnC-TnI^{DAN}-TnT)–Tm–F-$actin^{DAB}$] method-of-moments analyses (Table 1). Top panels show the difference function D for the (TnC-TnI^{DAN}-TnT)–Tm–F-$actin^{DAB}$ data, where $D = (I_{c,i} - I_{e,i})/(I_{e,i})^{1/2}$, and where $I_{c,i}$ and $I_{e,i}$ are calculated and experimental fluorescence intensities, respectively, in the ith channel. Tn subunits, Tm, actin, and myosin subfragment-1 were prepared as described (*16–18*). TnI was labeled with 1,5-IAEDANS by a procedure (*13*) that has been shown to label only Cys^{133} (*19, 20*). Actin was labeled at Cys^{374} with DAB-Mal as described (*15*). Sample buffer was 2 m*M* Hepes (*p*H 7.5), 50 m*M* NaCl, and 0.2 m*M* adenosine triphosphate (ATP) and contained 0.2 m*M* $CaCl_2$ (for the Ca^{2+}-state), or 0.2 m*M* $CaCl_2$ and 2 m*M* EGTA (for the apo-state), or 0.2 m*M* $CaCl_2$, 2 m*M* EGTA, and 4 m*M* $MgCl_2$ (for the Mg^{2+}-state). Fluorescence decay measurements (*21*) were made at 25°C on the same samples by successively adding $CaCl_2$, EGTA, and $MgCl_2$.

In a parallel experiment, TnI was labeled at Cys^{133} with the photoactivatable cross-linker BP-Mal (benzophenone-4-maleimide) and actin was fluorescently tagged with the reagent CP-Mal [3-(4-maleimidylphenyl)-7-diethylamino-4-methylcoumarin]. The reconstituted (TnC-TnI^{BP}-TnT)–Tm–F-$actin^{CP}$ thin filament was irradiated with ultraviolet light in the presence or absence of Ca^{2+} (presence of Mg^{2+}). Whereas little or no photo cross-linking occurred in the presence of Ca^{2+}, a cross-linked product between TnI and actin was observed after 5 min of irradiation in the absence of Ca^{2+} (Fig. 2). Further irradiation up to 30 min yielded no significant changes either in the presence or absence of Ca^{2+}. This result shows that the region of TnI containing Cys^{133} is within 9 Å (the length of the cross-linker) of some portion of actin in the absence of Ca^{2+}, but moves away from actin when Ca^{2+} binds to TnC. Experiments with TnI labeled with a nonspecific photo cross-linker showed a decrease in the extent of photo cross-linking with actin in the presence of Ca^{2+} (*11*). Our finding is consistent with this result, and identifies Cys^{133} and its vicinity as a region of TnI that undergoes Ca^{2+}-dependent interaction with actin.

We measured the Ca^{2+}-dependent Mg-ATPase activity (*12*) of myosin subfragment-1 in the presence of thin filaments reconstituted with labeled and unlabeled components to assess possible effects of the

Table 1. Fluorescence decay parameters of the TnI-bound donor 1,5-IAEDANS in the absence and presence of the F-actin–bound DAB-Mal acceptor. τ, Fluorescence lifetime in nanoseconds; A, fractional amplitude. Fluorescence decay curves (Fig. 1) were analyzed by the method-of-moments with the program FLUOR (*14*). One-component decays were obtained for the (TnC-TnI^{DAN}-TnT)–Tm–F-actin samples; two-exponential analysis yielded a second component of negligible amplitude. Two-component decays were obtained for the (TnC-TnI^{DAN}-TnT)–Tm–F-$actin^{DAB}$ samples; three-exponential analysis yielded a third component of negligible amplitude. Measurements were made in the Ca^{2+}-state (0.2 m*M* $CaCl_2$), apo-state (0.2 m*M* $CaCl_2$, 2 m*M* EGTA), and Mg^{2+}-state (0.2 m*M* $CaCl_2$, 2 m*M* EGTA, 4 m*M* $MgCl_2$). Other conditions are specified in Fig. 1. Standard deviations of ~0.1 ns and ~0.5 ns for lifetimes derived from one- and two-exponential decays, respectively, were estimated by repeating some of the measurements more than three times.

Material	A_1	τ_1 (ns)	A_2	τ_2 (ns)	A_3	τ_3 (ns)
(TnC-TnI^{DAN}-TnT)–Tm–F-actin, Ca^{2+}	1.000	15.52				
	0.998	15.38	0.002	39.95		
(TnC-TnI^{DAN}-TnT)–Tm–F-$actin^{DAB}$, Ca^{2+}	0.951	13.62	0.049	22.91		
	0.767	12.44	0.228	18.51	0.005	−7.82
(TnC-TnI^{DAN}-TnT)–Tm–F-actin, Mg^{2+}	1.000	17.14				
	1.000	17.14	7.35×10^{-8}	−410		
(TnC-TnI^{DAN}-TnT)–Tm–F-$actin^{DAB}$, Mg^{2+}	0.733	8.71	0.267	18.00		
	0.726	8.60	0.274	17.90	1.75×10^{-4}	−13.60
(TnC-TnI^{DAN}-TnT)–Tm–F-actin, apo	1.000	17.10				
	1.000	17.05	2.75×10^{-4}	85.93		
(TnC-TnI^{DAN}-TnT)–Tm–F-$actin^{DAB}$, apo	0.647	7.15	0.353	16.92		
	0.648	7.16	0.352	16.93	6.4×10^{-7}	69.56

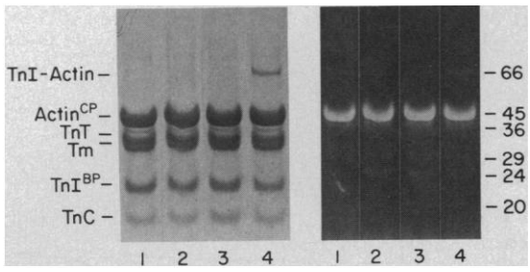

Fig. 2. Polyacrylamide (12.5%) gel electrophoresis showing photo cross-linking between TnI and actin in the reconstituted (TnC-TnI^{BP}-TnT)–Tm–F-actin^{CP} thin filament system in the presence (lanes 1 and 2) or absence (lanes 3 and 4) of Ca^{2+}. (Lanes 1 and 3) Samples before irradiation; (lanes 2 and 4) samples that have been irradiated for 5 min at 4°C. (Left panel) The Coomassie blue–stained gel; (right panel) the fluorescence of the same gel before staining. Labeling of TnI with BP-Mal and of actin with CP-Mal were performed as described in Fig. 1. Samples irradiated (*22*) in the presence of Ca^{2+} contained 0.2 m*M* $CaCl_2$; those irradiated in the absence of Ca^{2+} contained 2 m*M* EGTA and 4 m*M* $MgCl_2$. The positions of molecular mass markers (in kilodaltons) are shown on the right.

modifications on the activity. The regulatory capacity values [defined as $1 - (Act_{Ca^{2+}}/Act_{EGTA})$, where $Act_{Ca^{2+}}$ and Act_{EGTA} are Mg-ATPase activities in the presence and absence of Ca^{2+}, respectively] of (TnC-TnI-TnT)–Tm–F-actin, (TnC-TnI^{DAN}-TnT)–Tm–F-actin^{DAB}, and (TnC-TnI^{BP}-TnT)–Tm–F-actin^{CP} were 0.60, 0.55, and 0.71, respectively (duplicate measurements yielded values of 0.62, 0.61, and 0.65, respectively). Thus, the modifications do not significantly affect the regulatory capacity of the reconstituted thin filaments.

Our energy transfer and photo cross-linking results provide evidence that the protein region containing Cys^{133} of TnI is in close proximity to actin in the absence of Ca^{2+} and moves away from actin in the presence of Ca^{2+}. This movement is most likely induced by the binding of Ca^{2+} to the low-affinity "triggering" sites of TnC, although the possibility of its induction by Ca^{2+} replacing Mg^{2+} at the high-affinity sites cannot be ruled out at present. We have shown that in the ternary Tn complex, the same region of TnI moves toward Cys^{98} of TnC in response to Ca^{2+} (*13*). Thus, the Cys^{133} region of TnI appears to switch between actin and TnC in such a manner that it is close to actin when Ca^{2+} is absent and moves away from actin toward TnC when Ca^{2+} binds to TnC. These results are consistent with the proposed model for Ca^{2+} regulation of striated muscle contraction and confirm the role that TnI plays as a Ca^{2+}-dependent molecular switch in thin filament–based regulation.

Table 2. Parameters of energy transfer between the 1,5-IAEDANS donor and the DAB-Mal acceptor in the reconstituted (TnC-TnI^{DAN}-TnT)–Tm–F-actin^{DAB} thin filament complex as a function of the different metal-binding states. τ_d and τ_{da}, Donor fluorescence lifetimes (in nanoseconds) in the absence and presence of acceptor, respectively; E, transfer efficiency defined as $E = 1 - (\tau_{da}/\tau_d)$; ϕ_d, donor quantum yield; R_o, critical transfer distance obtained under the assumption that $\kappa^2 = 2/3$; R, apparent donor-acceptor separation distance. The lifetimes of (TnC-TnI^{DAN}-TnT)–Tm–F-actin were taken to be τ_d, whereas those of the major component of (TnC-TnI^{DAN}-TnT)–Tm–F-actin^{DAB} were taken to be τ_{da} (Table 1). ϕ_d was calculated as $\phi_d = \phi_d'(\tau_d/\tau_d')$ with values of $\phi_d' = 0.53$ and $\tau_d' = 13.5$ ns, where ϕ_d' and τ_d' are the fluorescence quantum yield and lifetime, respectively, of the 1,5-IAEDANS–labeled αα isoform of Tm (*15*). R_o was calculated as $R_o = R_o'(\tau_d/\tau_d')^{1/6}$, with the value of $R_o' = 39.9$ Å, where R_o' is the critical transfer distance for the 1,5-IAEDANS–DAB-Mal couple attached to ααTm and F-actin, respectively (*15*). R was calculated from the equation $R = R_o(E^{-1} - 1)^{1/6}$.

Metal-binding state	τ_d (ns)	τ_{da} (ns)	E	ϕ_d	R_o (Å)	R (Å)
Ca^{2+}	15.52	13.62	0.122	0.61	40.8	56.7
Mg^{2+}	17.14	8.71	0.492	0.67	41.5	41.7
Apo	17.10	7.15	0.582	0.67	41.5	39.3

REFERENCES AND NOTES

1. S. Ebashi and M. Endo, *Prog. Biophys. Mol. Biol.* **18**, 123 (1968).
2. M. L. Greaser and J. Gergely, *J. Biol. Chem.* **246**, 4226 (1971).
3. S. V. Perry, H. Cole, J. F. Head, F. J. Wilson, *Cold Spring Harbor Symp. Quant. Biol.* **37**, 251 (1972).
4. J. D. Potter and J. Gergely, *Biochemistry* **13**, 2697 (1974).
5. S. E. Hitchcock, *Eur. J. Biochem.* **52**, 255 (1975).
6. Z. Grabarek and J. Gergely, *Acta Biochim. Biophys. Hung.* **22**, 307 (1987).
7. S. S. Margossian and C. Cohen, *J. Mol. Biol.* **81**, 409 (1973).
8. S. E. Hitchcock, H. E. Huxley, A. G. Szent-Györgyi, *ibid.* **80**, 825 (1973).
9. T. Tao, B.-J. Gong, P. C. Leavis, unpublished observations.
10. L. Stryer, *Annu. Rev. Biochem.* **47**, 819 (1978).
11. K. Sutoh and F. Matsuzaki, *Biochemistry* **19**, 3878 (1980).
12. H. D. White, *Methods Enzymol.* **85**, 698 (1982).
13. T. Tao, E. Gowell, G. M. Strasburg, J. Gergely, P. C. Leavis, *Biochemistry* **28**, 5902 (1989).
14. E. W. Small and I. Isenberg, *Biopolymers* **15**, 1093 (1976).
15. T. Tao, M. L. Lamkin, S. S. Lehrer, *Biochemistry* **22**, 3059 (1983).
16. M. L. Greaser and J. Gergely, *J. Biol. Chem.* **248**, 2125 (1973).
17. J. A. Spudich and S. Watt, *ibid.* **246**, 4866 (1971).
18. A. G. Weeds and B. Pope, *J. Mol. Biol.* **111**, 129 (1977).
19. P. C. S. Chong and R. S. Hodges, *J. Biol. Chem.* **257**, 2549 (1982).
20. G. M. Strasburg, P. C. Leavis, J. Gergely, *ibid.* **260**, 366 (1985).
21. T. Tao and J. Cho, *Biochemistry* **18**, 2759 (1979).
22. T. Tao, M. Lamkin, C. J. Scheiner, *Arch. Biochem. Biophys.* **240**, 627 (1985).

23. We thank J. Gergely and Z. Grabarek for advice and discussions. Supported by NIH grants to T. Tao (AR21673) and P. C. Leavis (HL20464) and by the Muscular Dystrophy Association.

24 October 1989; accepted 24 January 1990

Hypoxic Dilation of Coronary Arteries Is Mediated by ATP-Sensitive Potassium Channels

JÜRGEN DAUT, WILLIBALD MAIER-RUDOLPH, NIKOLAS VON BECKERATH, GERHARD MEHRKE, KERSTIN GÜNTHER, LISELOTTE GOEDEL-MEINEN

The function of the heart depends critically on an adequate oxygen supply through the coronary arteries. Coronary arteries dilate when the intravascular oxygen tension decreases. Hypoxic vasodilation in isolated, perfused guinea pig hearts can be prevented by glibenclamide, a blocker of adenosine triphosphate (ATP)–sensitive potassium channels, and can be mimicked by cromakalim, which opens ATP-sensitive potassium channels. Opening of potassium channels in coronary smooth muscle cells and the subsequent drop in intracellular calcium is probably the major cause of hypoxic and ischemic vasodilation in the mammalian heart.

BLOOD FLOW THROUGH THE CORONARY arteries is precisely regulated, and any imbalance between the oxygen supply and the oxygen demand of the heart leads to angina pectoris or to heart failure. A decrease of the oxygen tension in coronary arteries (hypoxia) or an interruption of blood flow (ischemia) causes a marked reduction of the resistance of coronary arteries. The proposed mechanisms underlying this dilation of coronary arteries

J. Daut, N. von Beckerath, G. Mehrke, K. Günther, Physiologisches Institut der Technischen Universität München, Biedersteiner Strasse 29, D-8000 München 40, Federal Republic of Germany.
W. Maier-Rudolph and L. Goedel-Meinen, 1. Medizinische Klinik, Klinikum rechts der Isar der Technischen Universität München, D-8000 München 80, Federal Republic of Germany.